CHAPTER ONE

Direct Fluorescent Imaging of Translocation and Unwinding by Individual DNA Helicases

T.L. Pavankumar[1], **J.C. Exell**[1], **S.C. Kowalczykowski**[2]
University of California, Davis, CA, United States
[2]Corresponding author: e-mail address: sckowalczykowski@ucdavis.edu

Contents

[1] Both authors contributed equally to this work.

Methods in Enzymology, Volume 581
ISSN 0076-6879
http://dx.doi.org/10.1016/bs.mie.2016.09.010

Abstract

The unique translocation and DNA unwinding properties of DNA helicases can be concealed by the stochastic behavior of enzyme molecules within the necessarily large populations used in ensemble experiments. With recent technological advances, the direct visualization of helicases acting on individual DNA molecules has contributed significantly to the current understanding of their mechanisms of action and biological functions. The combination of single-molecule techniques that enable both manipulation of individual protein or DNA molecules and visualization of their actions has made it possible to literally see novel and unique biochemical characteristics that were previously masked. Here, we describe the execution and use of single-molecule fluorescence imaging techniques, focusing on methods that include optical trapping in conjunction with epifluorescent imaging, and also surface immobilization in conjunction with total internal reflection fluorescence visualization. Combined with microchannel flow cells and microfluidic control, these methods allow individual fluorescently labeled protein and DNA molecules to be imaged and tracked, affording measurement of DNA unwinding and translocation at single-molecule resolution.

1. INTRODUCTION

In this chapter, we describe methods to visualize DNA and proteins at the single-molecule level. Ensemble biochemical analyses have contributed considerably to an understanding of DNA unwinding and translocation behavior of helicases and motor proteins (Byrd & Raney, 2012; Gilhooly, Gwynn, & Dillingham, 2013; Lohman, Tomko, & Wu, 2008; Pyle, 2008; Singleton, Dillingham, & Wigley, 2007; Spies, Dillingham, & Kowalczykowski, 2005). Though important, these methods measure the average behavior of an ensemble of molecules. A complete understanding requires direct measurement of individual events that make up the distribution of behaviors that comprise the ensemble. In recent decades, we have used single-molecule imaging to visualize the movement and actions of DNA motor proteins (Amitani, Baskin, & Kowalczykowski, 2006; Bianco et al., 2001; Handa, Bianco, Baskin, & Kowalczykowski, 2005; Liu, Baskin, & Kowalczykowski, 2013; Nimonkar, Amitani,

Baskin, & Kowalczykowski, 2007; Rad, Forget, Baskin, & Kowalczykowski, 2015; Spies, Amitani, Baskin, & Kowalczykowski, 2007; Spies et al., 2003; Amitani, Liu, Dombrowski, Baskin, & Kowalczykowski, 2010; Forget, Dombrowski, Amitani, & Kowalczykowski, 2013; Hilario & Kowalczykowski, 2010; Sun & Wang, 2016). Here, we limit ourselves to a description of some of those methods. However, the study of protein–DNA interactions at the single-molecule level is supported by a wide range of complementary techniques, including, but not limited to, atomic force microscopy, electron microscopy, force spectroscopy, fluorescence correlation spectroscopy, Förster resonance energy transfer, magnetic tweezers, optical traps combined with fluorescence microscopy, and total internal reflection fluorescence (TIRF) microscopy (Bustamante, Bryant, & Smith, 2003; Greenleaf, Woodside, & Block, 2007; Ha, Kozlov, & Lohman, 2012; Kapanidis & Strick, 2009; Lionnet et al., 2012; Moffitt, Chemla, Smith, & Bustamante, 2008; Neuman & Nagy, 2008; Qi & Greene, 2016; Roy, Hohng, & Ha, 2008; Spies, 2013; Yodh, Schlierf, & Ha, 2010). Mechanical manipulation of individual DNA molecules by optical trapping of attached microspheres or by attachment to a surface has been a useful platform for studying the mechanisms of DNA helicases and translocases (Amitani et al., 2006, 2010; Bianco et al., 2001; Forget et al., 2013; Hilario & Kowalczykowski, 2010; Liu et al., 2013; Rad et al., 2015; Sun & Wang, 2016).

Imaging that employs optical trapping typically uses a laser trap to physically restrain a polystyrene bead that is attached to one end of a DNA molecule. The normally coiled DNA is extended either by force generated from solution flow (Perkins, Quake, Smith, & Chu, 1994; Perkins, Smith, & Chu, 1994) or by attachment of the free end to a second bead, which is captured by a second distal optical trap (Forget et al., 2013; Forget & Kowalczykowski, 2012). The now extended DNA is visualized by fluorescent dyes whose quantum yield is enhanced by binding to double-stranded DNA (dsDNA) (Bianco et al., 2001; Perkins, Quake, et al., 1994; Perkins, Smith, & Chu, 1994).

In TIRF microscopy, DNA–protein interactions are studied by attachment of either the DNA or the protein to a functionalized surface. The use of TIRF allows selective illumination of a region extending ~100–200 nm from the glass surface, enabling excitation of molecules only within this region (Axelrod, 1989). This selectivity greatly improves visualization of fluorescently labeled DNA or protein molecules attached, or near, to the surface, minimizing background fluorescence from the bulk solution, thereby increasing the signal over background.

In this review, we describe the instrumentation and experimental techniques required to image DNA helicases and translocases at the single-molecule level. In particular, we describe methods that allow visualization of the movement of these motor proteins, or their unwinding activity, using direct or indirect fluorescent labeling procedures. The usefulness of the aforementioned techniques was demonstrated in studies of *Escherichia coli* RecBCD and RecQ helicases. These two enzymes will serve as the prototypes for elaborating the procedures required for fluorescent visualization using optical trapping and TIRF, respectively. Although described specifically for RecBCD and RecQ, these approaches can be, and have been, successfully adapted for use with other DNA helicases and translocases (Amitani et al., 2006; Nimonkar et al., 2007; Reuter, Parry, Dryden, & Blakely, 2010).

1.1 RecBCD Function and Properties

RecBCD enzyme is a 330 kDa heterotrimeric protein complex involved in homologous recombination (Dillingham & Kowalczykowski, 2008). It is a combined helicase/nuclease that catalyzes DNA end resection by producing single-stranded DNA (ssDNA) during recombinational repair of double-strand DNA breaks. It is a bipolar helicase containing two DNA motor subunits (RecB and RecD) with opposite translocation polarities (Dillingham, Spies, & Kowalczykowski, 2003; Taylor & Smith, 2003). RecBCD is an extremely fast (1–2 kb/s) and highly processive enzyme (~30 kb per binding event) (Roman, Eggleston, & Kowalczykowski, 1992). During DNA end resection, RecBCD recognizes an octameric DNA sequence, 5′-GCTGGTGG-3′, called Chi (crossover hot spot instigator). Recognition of Chi alters the enzyme's biochemical properties, attenuating its nuclease activity (Dillingham & Kowalczykowski, 2008; Dixon & Kowalczykowski, 1993).

Single-molecule studies using an optical tweezer combined with fluorescence microscopy have revealed interesting and unprecedented biochemical properties of RecBCD that could not be determined using traditional ensemble biochemical methods. In brief, an optical trap was used to capture a single-DNA molecule to which RecBCD was bound (Bianco et al., 2001; Handa et al., 2005; Spies et al., 2003, 2007), and DNA unwinding was imaged by using fluorescent reporter molecules that either were bound to duplex DNA and were displaced upon unwinding (Bianco et al., 2001) (Fig. 1 and Movie 1 (http://dx.doi.org/10.1016/bs.mie.2016.09.010)), or were attached to the enzyme itself as it moved along the DNA

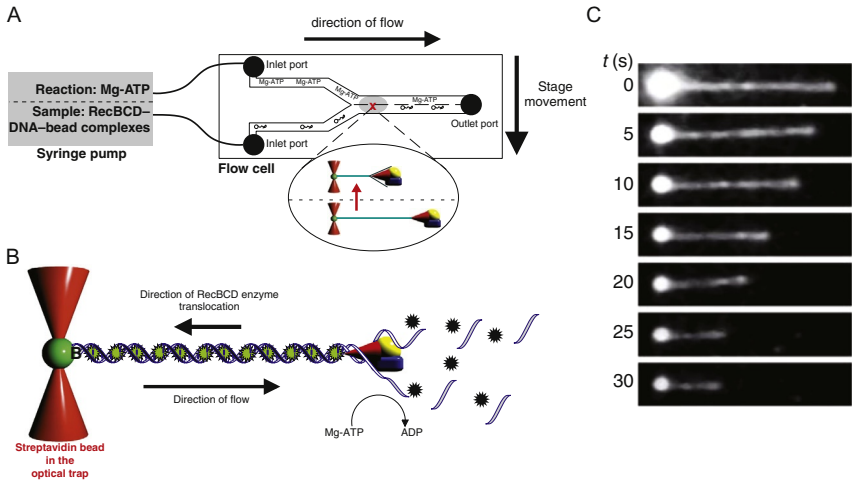

Fig. 1 Schematic representation of a multichannel flow cell used for visualization of DNA unwinding by an individual RecBCD enzyme. (A) Two-channel flow cell connected to a syringe pump. First channel contains RecBCD–DNA–bead complex and the second channel, the "reaction channel" contains ATP. "X" indicates the position of the optical trap, and this region is magnified to show movement of the enzyme-DNA–bead complex to the reaction channel. The RecBCD–DNA–bead complex is moved into the reaction channel by moving the stage by 400 μm. (B) The optically trapped fluorescently labeled dsDNA is extended by flow and its observed length decreases as RecBCD unwinds and degrades it. (C) Sequential images of DNA shortening as a function of time (*t*, in seconds) by RecBCD. *Panels (A) and (B): From Bianco, P. R., Brewer, L. R., Corzett, M., Balhorn, R., Yeh, Y., Kowalczykowski, S. C., & Baskin, R. J. (2001). Processive translocation and DNA unwinding by individual RecBCD enzyme molecules.* Nature, 409*(6818), 374–378. doi:10.1038/35053131. Panel (C): From Liu, B., Baskin, R. J., & Kowalczykowski, S. C. (2013). DNA unwinding heterogeneity by RecBCD results from static molecules able to equilibrate.* Nature, 500*(7463), 482–485. http://dx.doi.org/10.1038/nature12333.*

(Handa et al., 2005) (Fig. 2 and Movie 2 (http://dx.doi.org/10.1016/bs.mie.2016.09.010)). Using phage λ DNA containing a Chi sequence as a DNA substrate, RecBCD enzyme was seen to pause at Chi (for several seconds) but then resumed translocation afterward at a reduced rate, approximately one-half the pre-Chi rate (Spies et al., 2003). Furthermore, single-molecule analysis of RecBCD enzymes mutated in individual motor subunits revealed that the change in translocation rate was indeed due to switching of lead motor utilization, from RecD to RecB, upon Chi recognition (Spies et al., 2007). The heterogeneity in translocation velocities manifested by the RecBCD helicase is attributed to ergodic behavior by the enzyme (Liu et al., 2013).

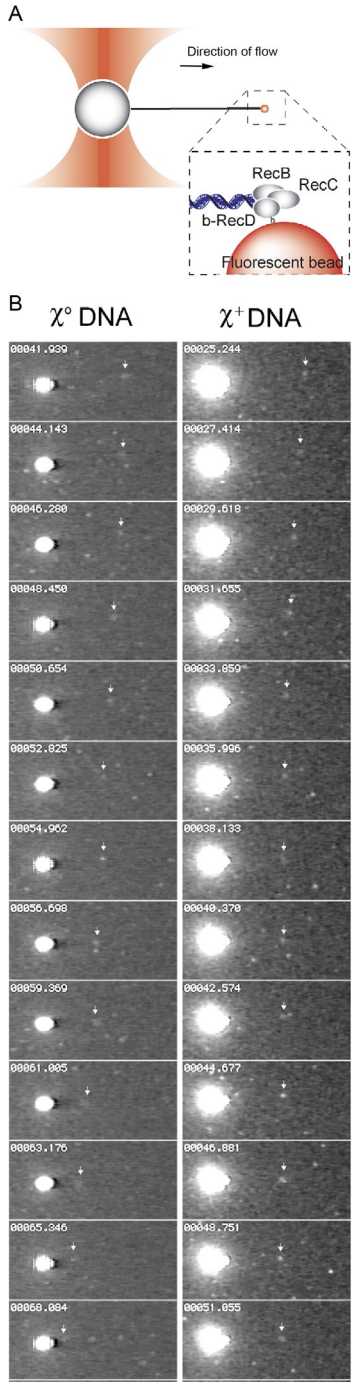

Fig. 2 See legend on opposite page.

1.2 RecQ Function and Properties

A different approach was used to monitor DNA unwinding by *E. coli* RecQ helicase, which is the founding member of the ubiquitous class of RecQ-like helicases (Chu & Hickson, 2009). The unwinding behavior of RecQ is dynamic (Harmon & Kowalczykowski, 2001; Rad & Kowalczykowski, 2012a, 2012b), requiring high concentrations of RecQ and ssDNA-binding (SSB) proteins. Consequently, surface immobilized DNA and visualization by TIRF were used to permit rapid and continuous exchange of DNA-bound proteins with those in the bulk solution. DNA unwinding by RecQ was visualized using a fluorescently modified SSB that served as a biosensor to directly detect ssDNA formation (Fig. 3). TIRF imaging was used to see the ssDNA unwinding tracts and the progression of unwinding forks in real time (Rad et al., 2015) (Fig. 4).

RecQ is a 3′–5′ helicase that participates in DNA-break repair by the RecF pathway of homologous recombination (Umezu, Nakayama, & Nakayama, 1990). In vivo, RecQ and RecJ, a 5′–3′ exonuclease, predominantly enlarge ssDNA gaps (Courcelle & Hanawalt, 1999), but can also resect dsDNA breaks into ssDNA needed for subsequent steps of homologous recombination (Handa, Morimatsu, Lovett, & Kowalczykowski, 2009; Morimatsu & Kowalczykowski, 2014). In vitro, RecQ can unwind a multitude of DNA substrates, requiring neither an ssDNA tail nor a dsDNA end from which to initiate unwinding (Harmon & Kowalczykowski, 1998, 2000, 2001; Umezu et al., 1990). Translocation occurs along ssDNA and this translocation is tightly coupled to DNA unwinding (Manosas, Xi, Bensimon, & Croquette, 2010; Rad & Kowalczykowski, 2012a; Sarlos, Gyimesi, & Kovacs, 2012). Single-molecule analysis of RecQ helicase

Fig. 2 Direct visualization of translocation by fluorescently labeled RecBCD enzyme. (A) Illustration of an optically trapped DNA molecule with fluorescently labeled RecBCD bound to the free end. The optically trapped dsDNA is extended by flow. In presence of ATP, the RecBCD enzyme (with fluorescent nanoparticle attached) translocates along the DNA from right to left, opposite to the direction of flow. (B) Sequential images of the RecBCD–nanoparticle complex translocating on two different DNA molecules, one devoid of Chi (*left*) and the other containing Chi (*right*). The intense bright spot on the left of each frame is the streptavidin-coated polystyrene bead, which is fluorescent due to nonspecific binding of the nanoparticles. The position of the RecBCD nanoparticle (*faint spot* to the *right*) is shown by an *arrow* in each frame. The numbers in image are an arbitrary time in seconds. *Panels (A) and (B): From Handa, N., Bianco, P. R., Baskin, R. J., & Kowalczykowski, S. C. (2005). Direct visualization of RecBCD movement reveals cotranslocation of the RecD motor after χ recognition.* Molecular Cell, 17*(5), 745–750. http://dx.doi.org/10.1016/j.molcel.2005.02.011*.

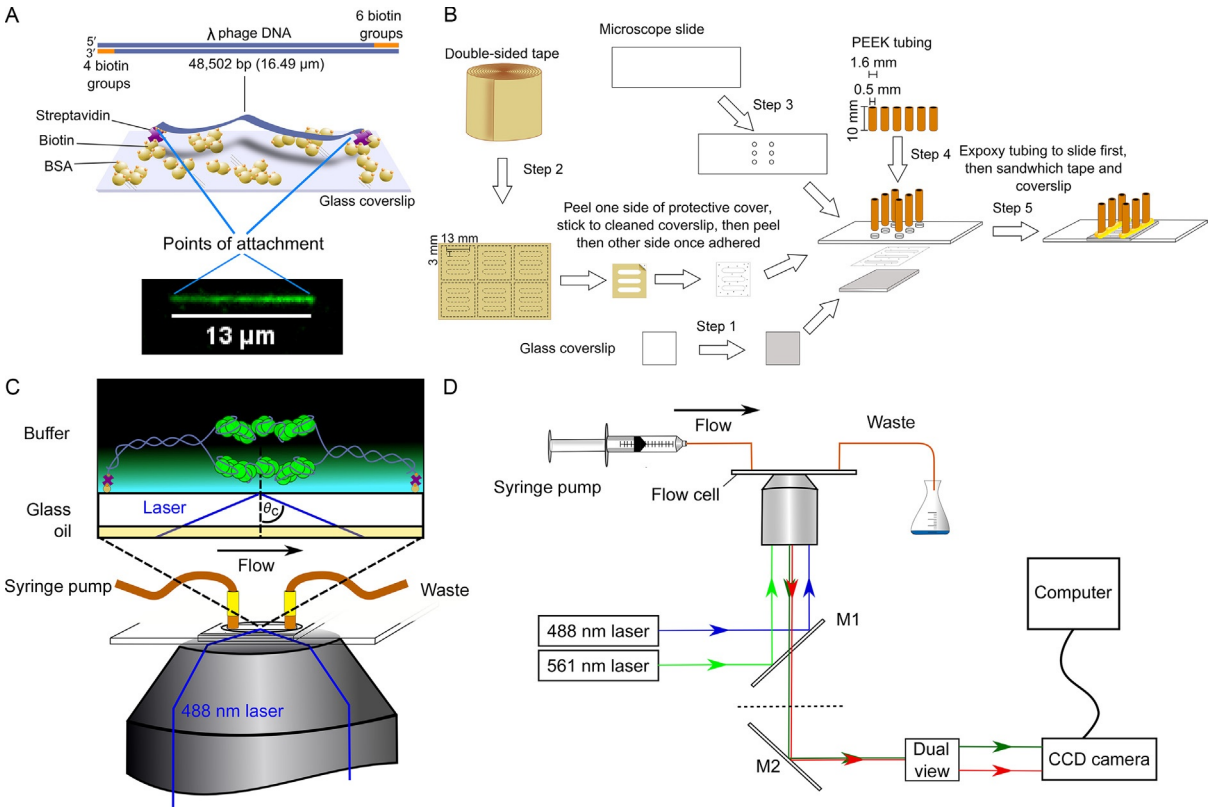

Fig. 3 See legend on opposite page.

activity showed that unwinding initiated with a dimer of RecQ locally melting dsDNA, and that processive unwinding of several kilobase pairs at maximal rates of ~40–60 bp/s involved multiple monomers at the DNA unwinding fork (Rad et al., 2015) (Movie 3 (http://dx.doi.org/10.1016/bs.mie.2016.09.010)). A microfluidic injection system, in combination with single-molecule TIRF, permitted rapid exchange of reaction components. As such, the unwinding rate could be measured in the absence of free RecQ (Movie 4 (http://dx.doi.org/10.1016/bs.mie.2016.09.010)). In this case, tracks of fluorescent SSB up to 2 kb were visualized from a single initiation event. Furthermore, it was demonstrated that unwinding could be reinitiated at a stalled unwinding fork. Such data, combined with the sigmoidal dependence of initiation events on protein concentration, suggested that multiple cooperating monomers of RecQ are required to efficiently unwind DNA (Byrd & Raney, 2015).

Using fluorescently modified SSB as a natural reporter of DNA unwinding activity has several advantages over the use of fluorescent dsDNA-binding dyes. Often, the fluorophore reduces the DNA helicase activity.

Fig. 3 Visualizing unwinding of individual DNA molecules using fluorescent SSB protein and TIRF microscopy. (A) *Top*: Diagram of phage λ DNA molecule with the indicated number of biotin groups incorporated in each 12-nt *cos* overhang. *Middle*: Illustration of biotinylated λ DNA attached at both ends via biotin–streptavidin linkage. *Bottom*: Image of an actual λ DNA molecule attached to the glass surface, stained with YO-PRO-1 (100 n*M*), and illuminated with a 488 nm laser. The image is false colored in *green* and the attachment points to the glass surface are indicated. (B) The process required to construct a flow cell containing three separate single-channels. The steps highlighted are equivalent to those described in Section 4.1. (C) The flow cell from (B) mounted onto the objective; biotinylated lambda DNA was injected under buffer flow, permitting attachment of both ends to the surface. Unwinding tracks are visualized by binding of AF488-SSB^{G26C} (*green*) to ssDNA regions. (D) Schematic representation of a TIRF microscope capable of visualizing DNA unwinding by RecQ by monitoring signal from both DNA and fluorescent SSB simultaneously. As shown in (C) the flow cell is mounted onto a 100× oil-immersion objective. The fluorescent SSB and DNA are excited by two lasers; 488 and 561 nm, respectively, and emission measured, via dichroic mirrors (M1 and M2). The deconvoluted emission is then directed onto different areas of a CCD camera generating a signal corresponding to either SSB or DNA. The lasers are operated using a custom LABview VI program to coordinate excitation with image acquisition so that the sample is illuminated only during the exposure times. *Panels (A) and (D): From Rad, B., Forget, A. L., Baskin, R. J., & Kowalczykowski, S. C. (2015). Single-molecule visualization of RecQ helicase reveals DNA melting, nucleation, and assembly are required for processive DNA unwinding.* Proceedings of the National Academy of Sciences of the United States of America, 112*(50), E6852–E6861. http://dx.doi.org/10.1073/pnas.1518028112.*

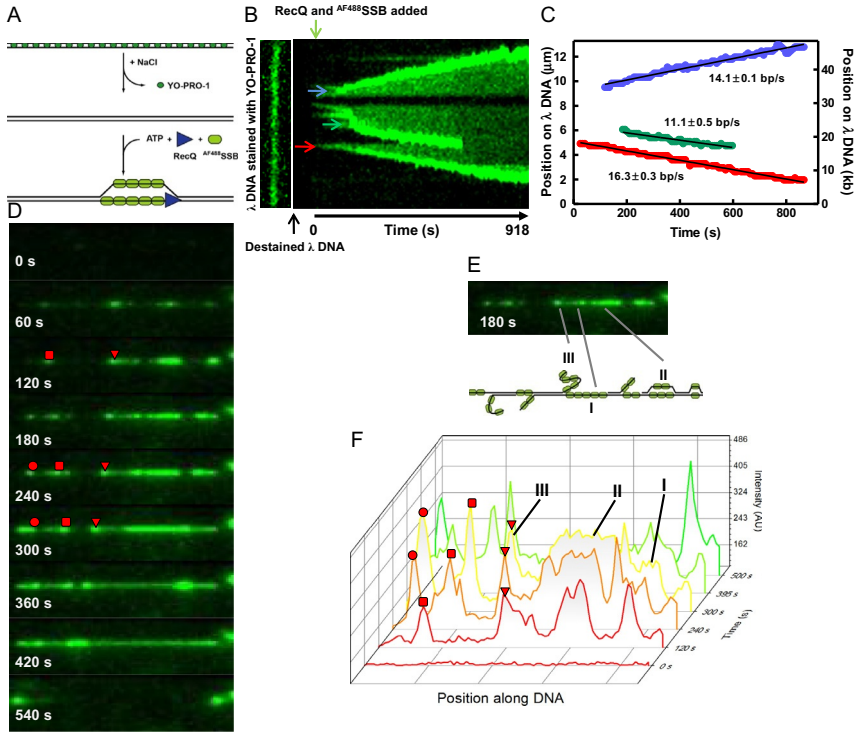

Fig. 4 Monitoring DNA unwinding by RecQ helicase using AF488-SSB^{G26C} as a sensor of ssDNA production. (A) Schematic of experiment employed to observe DNA unwinding by RecQ using signal from AF488-SSB^{G26C} bound to ssDNA. (B) Attachment to the surface at both ends of the λ DNA molecules is initially confirmed by staining dsDNA with YO-PRO-1. The stain is removed by washing with SMB2 containing 200 m*M* NaCl. *Left*, A doubly tethered λ DNA molecule stained with YO-PRO-1 (13.3 μm). *Right*: After destaining, RecQ (100 n*M*), ATP (1 m*M*), $Mg(OAc)_2$ (1 m*M*), and AF488-SSB^{G26C} (60 n*M*) in SMB2 are introduced into the flow cell; kymograph depicts three unwinding events on the same DNA molecule, each identified by AF488-SSB^{G26C} fluorescence. (C) The kymograph is analyzed using steps outlined in Section 7.2 to produce a graph showing position of unwinding forks in *B* vs time; *black line* is a fit to a linear region to obtain the unwinding rate. Error bars represent standard deviation. (D) Time-lapse images showing individual unwinding events on a single λ DNA molecule marked by bound AF488-SSB^{G26C}, in the presence of RecQ (80 n*M*). *Red circle*, *square*, and *triangle* highlight three unwinding forks tracked in F. (E) *Top*: The intensity per pixel due to AF488-SSB^{G26C} bound to unwound DNA can be used to determine different types of ssDNA products. Image shown is molecule in D after 180 s. *Bottom*: Interpretative diagram showing how different classes of unwound regions bound by AF488-SSB^{G26C} result in differences in their fluorescent intensity: class I, one strand of ssDNA; class II, unwinding bubbles with two strands of ssDNA; and class III, nicked ssDNA condensed by AF488-SSB^{G26C}. (F) The three unwinding forks highlighted in (D), *red circle*, *square*, and *triangle* are plotted as a

The level of inhibition is dependent on the dye and helicase, although judicious choice can yield unwinding rates that are essentially unaffected (Eggleston, Rahim, & Kowalczykowski, 1996; George, Ghate, Matson, & Besterman, 1992). The most significant drawback of fluorescent dyes is that they catalyze photocleavage of DNA (Akerman & Tuite, 1996). Although the newer generation of dyes (SYTOX or YO-PRO-1) has a significantly lower propensity to cause photocleavage compared to, for example, YOYO-1, they induce cleavage nonetheless.

1.3 SSB Function and Properties

In all cells, ssDNA is protected by the binding of a ssDNA-binding protein (Richard, Bolderson, & Khanna, 2009; Shereda, Kozlov, Lohman, Cox, & Keck, 2008). SSB proteins not only bind ssDNA but also interact with many different proteins to orchestrate DNA replication and repair processes. One group of these interacting partners is the DNA helicases. SSB proteins can stimulate the unwinding activity of helicases by direct interaction, by preventing DNA reannealing, or by sequestering ssDNA to which helicases can bind, preventing product inhibition (Cejka & Kowalczykowski, 2010; Harmon & Kowalczykowski, 2001; Umezu & Nakayama, 1993).

SSB from *E. coli* is a homotetramer. The DNA can bind and wrap around each monomer, and the extent of wrapping is dependent on the salt concentration, temperature, pH, and the ratio of SSB to ssDNA. As a result, the stoichiometry of ssDNA binding by SSB, referred to as "binding modes," is highly dependent on these variables (Lohman & Ferrari, 1994; Raghunathan, Kozlov, Lohman, & Waksman, 2000; Shereda et al., 2008). Two binding modes predominate. If conditions favor a binding mode where

function of pixel intensities along the contour of the unwound molecule. These traces are shown for six of the frames along the time-course in (D). The intensities of the three different classes of ssDNA bound by AF488-SSB^{G26C} are highlighted by *Roman numerals* and correspond to the structures shown in (E). Other details from RecQ unwinding can also been seen from these plots, the unwinding forks corresponding to the *red*, *triangle*, and *square* converge, as seen at 420 s in (D). In addition, the DNA molecule breaks internally at 500 s (*blue* trace). *Panels (A–F): From Rad, B., Forget, A. L., Baskin, R. J., & Kowalczykowski, S. C. (2015). Single-molecule visualization of RecQ helicase reveals DNA melting, nucleation, and assembly are required for processive DNA unwinding.* Proceedings of the National Academy of Sciences of the United States of America, 112*(50), E6852–E6861. http://dx.doi.org/10.1073/pnas.1518028112.*

DNA is bound to all four SSB subunits, then the tetramer occupies ~65 nucleotides (Lohman & Ferrari, 1994). Alternatively, if only two of the four monomers are bound to the DNA, then the tetramer binds ~35 nucleotides. Regardless of the binding mode, association of SSB and ssDNA is rapid and diffusion limited (Lohman & Ferrari, 1994). This is of paramount importance for their use in measuring DNA unwinding rates.

The first example of using SSB as a biosensor to follow DNA unwinding by a helicase took advantage of the decreased intrinsic tryptophan fluorescence of SSB upon binding to ssDNA (Roman & Kowalczykowski, 1989). The concept was then adapted to incorporate an extrinsic fluorophore into phage T4 ssDNA-binding protein, gp32 (Liu, Qian, & Morrical, 2006). This innovation improved the signal change upon binding and shifted the spectrum into the visible region. SSB was modified to directly measure unwinding by placing fluorescent dyes on residues near the ssDNA-binding domain (Dillingham et al., 2008). Each monomer contains oligosaccharide/oligonucleotide binding folds (OB-folds) that form groves along the protein's surface allowing ssDNA to bind. Taking advantage of the lack of natural cysteine residues in wild-type SSB, amino acid residues along these grooves were mutated individually to cysteine to permit coupling to fluorescent dyes. Placement of certain fluorophores at these sites produced a relatively large enhancement in the fluorescent signal upon binding to ssDNA. The initial study described a mutant protein, SSB^{G26C}, which had been reacted with a coumarin fluorophore, IDCC (*N*-[2-(iodoacetamido)ethyl]-7-diethylaminocoumarin-3-carboxamide) (Dillingham et al., 2008). The fluorescently labeled protein, DCC-SSB, was used to accurately determine the DNA unwinding rates of AddAB, RecBCD, and PcrA helicases. In a subsequent study, another variant, SSB^{W88C}, was coupled to Cy3b (Fili et al., 2010). This particular dye has significantly improved quantum yield and photostability, compared to previously used dyes, permitting the use of the fluorescent SSB in single-molecule experiments. Again, the rates of AddAB, RecBCD, and PcrA were measured, and it was demonstrated that Cy3b-SSB^{W88C} association with product ssDNA accurately reported on their rates of unwinding.

Here, this review concentrates on the use of fluorescently labeled SSB to image DNA unwinding by RecQ (Rad et al., 2015). The reagent is SSB^{G26C} conjugated with either Alexa Fluor 488 (AF488) or Alexa Fluor 546 (AF546) (Section 3.2). DNA unwinding is visualized by SSB binding and the concomitant appearance of fluorescence. By immobilizing λ dsDNA

that is elongated on a surface using microfluidics, tracks due to SSB binding can be seen initiating and physically growing as a product of RecQ activity. The formation and progression of individual unwinding forks is readily visualized. The rate, direction, and processivity of unwinding at individual forks can be determined using this method. The steps required to observe and quantify unwinding by RecQ using fluorescent SSB are outlined below.

2. PREPARATION OF DNA SUBSTRATES

In practical terms, fluorescence imaging techniques, such as the two described herein (epifluorescence and TIRF), require immobilization of either protein or DNA substrate to visualize their behaviors by optical microscopy. Typically, immobilization is achieved by modification of the DNA to permit its attachment to a bead or a surface. Bacteriophage λ DNA (48,502 bp in length) is a widely used dsDNA substrate to study the DNA unwinding and translocating properties of proteins in single-molecule experiments. The DNA ends are modified to allow binding of the DNA to a functionalized surface of choice. The modifications can be introduced at one or both ends of the λ DNA, which conveniently has unique 3′ recessed ends that are 12 nucleotides in length (the *cos* site). These *cos* sites permit annealing and subsequent ligation of modified oligonucleotides (Sections 2.1 and 2.2) or incorporation of modified nucleotides by a DNA polymerase (Section 2.3).

2.1 Preparation of λ DNA With a Biotinylated End by Ligation

Bacteriophage λ DNA (New England Biolabs (NEB), Ipswich, MA) has complementary 12 nucleotide ssDNA cohesive sites at each terminus (*cos* ends). Depending on which end needs to be biotinylated, a 3′-biotinylated 12-mer oligonucleotide (5′-GGGCGGCGACCT-3′ or 5′-AGGTCGCCGCCC-3′; Integrated DNA Technology, Coralville, IA) is ligated to an end.

1. Phosphorylate oligonucleotide by incubating 5 μ*M* 3′-biotinylated 12-mer oligonucleotides with 1 m*M* ATP and 0.2 U/μL polynucleotide kinase (PNK) in 50 μL PNK buffer (70 m*M* Tris–HCl (pH 7.6), 10 m*M* $MgCl_2$, and 5 m*M* DTT) at 37°C for 1 h.
2. Heat-inactivate the enzyme by incubating at 75°C for 10 min.
3. Add 15 n*M* (molecules) phosphorylated oligonucleotides to 25 ng/μL (0.75 n*M* molecules) of λ DNA (20:1 ratio) in a 90-μL reaction volume containing 100 m*M* NaCl.

Note: Care must be taken while handling phage λ DNA. Due to its long length, λ DNA is highly susceptible to shearing. Hence, the use of cut-off pipette tips (wide-mouth tips), gentle mixing (no vortexing), and low-speed centrifugation are recommended.

4. Carry out the annealing reaction with an initial incubation at 75°C for 15 min, followed by a stepwise decrease in temperature at 1°C/min using a PCR machine. Alternatively, annealing can be carried out by starting at 75°C for 15 min in a heating block. Later, by simply turning off the heated block, allow it to cool down slowly to room temperature (over at least 1 h).
5. Ligate the annealed oligo-λ DNA complex by adding 10 μL of 10× T4 DNA ligase buffer (500 m*M* Tris–HCl (pH 7.5), 100 m*M* $MgCl_2$, 10 m*M* ATP, and 100 m*M* DTT), and 1 μL of T4 DNA ligase (400 units) to the annealed (90 μL) reaction.
6. Incubate the reaction at 16°C overnight, or room temperature for 1 h.
7. Stop reaction by adding ethylenediaminetetraacetic acid (EDTA) to a final concentration of 10 m*M* and heat-inactivating the T4 DNA ligase for 10 min at 65°C.
8. Remove excess oligonucleotides and other components by gel filtration using a prepacked MicroSpin column (e.g., Illustra MicroSpin S-400 HR Columns, GE Healthcare, Piscataway, NJ) as per manufacturer's protocol.

2.2 Preparation of λ DNA With Biotinylated and Digoxiginated (DIG) Ends by Ligation

The two cohesive ends (cos sites) can be treated differently, as needed. In this protocol, the attachment of complementary biotinylated oligonucleotide to the *cosB* (*cosL*) end and complementary digoxiginated oligonucleotide to the *cosA* (*cosR*) end of the DNA is explained.

1. Incubate 25 ng/μL of λ DNA (~750 p*M*, DNA molecules) with 15 n*M* of phosphorylated (see Section 2.1, steps 1 and 2) and digoxiginated oligonucleotide, 5′-GGGCGGCGACCT-3′ (*cosA*) (Operon Technologies, Huntsville, AL) in a 90-μL reaction mixture containing 100 m*M* NaCl at 75°C for 15 min in a heat block.
2. Allow the heat block slowly to cool to room temperature (over at least 1 h).
3. Add 10 μL of 10× T4 DNA ligase and T4 DNA ligase to a final concentration 4 U/μL and incubate at room temperature for 1 h.
4. Heat-inactivate T4 DNA ligase for 10 min at 65°C.

5. Remove free oligonucleotides using MicroSpin S-400 spin column as per manufacturer's protocol.
6. Add 37.5 n*M* (50-fold molar excess over the λ DNA end and more than 2-fold molar excess over the *cosA* oligonucleotide) biotinylated oligonucleotide, 5′-AGGTCGCCGCCC-3′ (*cosB*), and 4 U/μL T4 DNA ligase; incubate for 1 h at room temperature.
7. Stop the reaction by adding EDTA to a final concentration of 10 m*M* and heat-inactivating T4 DNA ligase for 10 min at 65°C.
8. Remove excess of digoxiginated oligonucleotides using MicroSpin S-400 column.
9. Modified oligonucleotides ligated to λ DNA can be stored at 4°C for several months (do not freeze).

   Note: The same protocol can be used to either biotinylate or digoxiginate both DNA ends, using appropriate modified oligonucleotides.

2.3 Preparation of λ DNA With Biotinylated Ends by DNA Synthesis

Both *cos* ends of λ DNA can be modified with multiple biotin moieties at each DNA end. This protocol describes biotinylation by synthetic fill-in of the 3′ recessed ends using exo$^-$ T4 DNA polymerase (NEB, Ipswich, MA).

1. In 30 μL of 1× NEB buffer-2.1, set up a reaction mixture containing 5 μg of λ DNA and 100 μ*M* each of dATP, dTTP, dCTP, and biotin-11-dGTP; add three units of T4 DNA polymerase.
2. Incubate the reaction for 15 min at 12°C.
3. Terminate the reaction by adding EDTA to a final concentration of 10 m*M* and heat-inactivating the enzyme for 20 min at 75°C.
4. Dilute the reaction mixture to a final volume of 100 μL with water and remove free dNTPs using MicroSpin S-400 HR column.
5. Store biotinylated λ DNA at 4°C.

2.4 Construction of λ DNA Containing a Unique Sequence

In this protocol, we briefly explain the steps involved in construction of a λ DNA substrate containing a unique sequence, using the Chi sequence as an example. The phage λgt10 vector is used. Lambda gt10 DNA is 43.34 kb in length with a unique *Eco*RI restriction site within the λ repressor (*cI*) gene. It can accept DNA restriction fragments up to 7.5 kb in length with *Eco*RI ends.

1. Prepare 30 μL of reaction mixture containing 2 μg of λgt10 DNA, 40% polyethylene glycol (PEG) 8000, 1× T4 DNA ligase buffer, and 4 U/μL T4 DNA ligase. Incubate reaction mixture overnight at 16°C. This step helps to prevent spurious ligation in later steps of the protocol.
2. Precipitate ligated product by ethanol precipitation, dry, and resuspend in 20 μL of water.
3. Add ligated λ gt10 DNA to a reaction mixture containing 1× CutSmart buffer (20 m*M* Tris–acetate (pH 7.9), 50 m*M* KOAc, 10 m*M* magnesium acetate, and 100 μg/mL bovine serum albumin (BSA)) and 0.5 U/μL *Eco*RI-HF restriction enzyme (NEB). Incubate for 2 h at 37°C.
4. Precipitate the DNA with ethanol, air dry, and suspend in 10 μL of 10 m*M* Tris–HCl (pH 8.0).
5. Prepare dsDNA with the desired sequence in any *Eco*RI-digested DNA fragment (e.g., for a Chi sequence, use *Eco*RI-digested pSNH33 (Spies et al., 2003)).

   Note: dsDNA containing any sequence of interest, up to 7.5 kb can be inserted.
6. Perform a ligation reaction, as described in Section 2.3, step 1, using a ratio of vector to insert of 1:10.
7. The ligated recombinant λ DNA product is packaged into a λ capsid in vitro using the Packagene® Lambda DNA Packaging System (Promega, Madison, WI).
8. Screen for the desired λ DNA recombinants using *E. coli* C600 *hflA* or any suitable host strain.

   Note: An *E. coli* strain inactivated for *hflA* is critical for maintaining the lysogenic mode of phage λ and is important for the recombinant screening process.
9. Make recombinant λ DNA stock using standard λ DNA isolation protocol (e.g., using the QIAGEN Lambda Purification Kit per manufacturer's instructions (Spies et al., 2003)).
10. Store the purified recombinant λ DNA at 4°C.

3. FLUORESCENT LABELING OF PROTEINS

Single-molecule imaging of individual proteins requires fluorescent modification to permit direct visualization. The ability to label proteins with a fluorophore without altering function is paramount for single-molecule imaging. Various techniques and methods are available to covalently link fluorophores to the protein of interest—too many to be considered here

(see, e.g., Chakraborty, Wang, Ebright, & Ebright, 2010; Hein et al., 2010; Kapanidis, Ebright, & Ebright, 2001; Shaner, Steinbach, & Tsien, 2005; Witte et al., 2013; Wu, Piatkevich, Lionnet, Singer, & Verkhusha, 2011). Here, we provide procedures for attachment of nanoparticles via biotinylated protein and for chemical labeling directly via amino or sulfhydryl groups.

3.1 Labeling of RecBCD Enzyme With a Fluorescent Nanoparticle

Here, we describe the technique used to directly visualizing individual RecBCD molecules translocating on single molecules of DNA. Real-time visualization of translocation was achieved by incorporating a biotin tag into a genetically modified RecBCD enzyme in vivo, and, then binding a streptavidin-coated fluorescent nanoparticle to the purified protein (Handa et al., 2005). As an alternative to nanoparticles, quantum dots can be substituted (Finkelstein, Visnapuu, & Greene, 2010).

1. Mix 4.8 μL of 1.22 μ*M* biotinylated RecBCD enzyme (stored in 20 m*M* Tris–HCl (pH 7.5), 0.1 m*M* EDTA, 0.1 m*M* DTT, 100 m*M* NaCl, and 50%, v/v glycerol) with 3 μL of streptavidin-coated florescent nanoparticle (~18 n*M*) (40 nm TransFluoSpheres; excitation 488 nm; emission 645 nm; Molecular Probes, Carlsbad, CA) in 50 m*M* sodium phosphate (pH 7.5), 50 m*M* NaCl, and 0.02% (v/v) Tween 20. Expression and purification of biotinylated RecBCD is elaborated elsewhere (Handa et al., 2005).

   Note: An excess of RecBCD over the bead concentration is necessary due to nonspecific loss of protein in the procedure.
2. Incubate for 10 min at 37°C and RecBCD–nanoparticles are ready to use with DNA–bead complex (proceed to Section 5.2, step 4).

3.2 Fluorescent Labeling of SSB, Used to Detect ssDNA

Proteins can be labeled relatively specifically at their N-terminus in a pH-controlled reaction that occurs between primary amines and a fluorophore that has been functionalized with a succinimidyl ester. This "N-terminal" labeling procedure has proven successful for covalently attachment of a fluorophore to a variety of proteins, RecA (Bell, Plank, Dombrowski, & Kowalczykowski, 2012; Galletto, Amitani, Baskin, Kowalczykowski, 2006), RAD51 (Hilario, Amitani, Baskin, & Kowalczykowski, 2009), and RPA2 (*Ferroplasma acidarmanus* SSB) (Honda, Park, Pugh, Ha, & Spies, 2009). However, the same method could not be used with *E. coli* SSB because the resultant protein had attenuated DNA-binding properties. Therefore, an alternative

strategy was adopted whereby residues at various positions were mutated to cysteine. The sulfhydryl group of cysteine was then coupled to iodoacetamide or maleimide functionalized dyes, resulting in formation of a thioether linkage. Here, we describe fluorescent labeling of SSB^{G26C}, with either AF 488 or AF 546 using maleimide chemistry.

1. Prepare 1 L of buffer containing 20 m*M* Tris–acetate (pH 7.5), 500 m*M* NaCl, 1 m*M* EDTA, and 20% (v/v) glycerol. Before use, filter the buffer through 0.22 μm filter membrane.
2. Take the desired amount of SSB^{G26C} (1 mL of 1.7 mg/mL, ~90 μ*M*) and dialyze against a minimum of 100-fold volume of buffer, twice, each dialysis for at least 4 h. The DTT or 2-mercaptoethanol (2-ME) from the storage buffer will compete for reaction with the dye; hence the dialysis (or spin column) step is essential to remove the DTT or 2-ME (or any reactive thiols) from the storage buffer.
3. Measure the concentration of SSB^{G26C} after dialysis. Add a 10-fold molar excess of Alexa Fluor 488-C_5 maleimide or Alexa Fluor 546-C_5 maleimide (Molecular Probes, Eugene, OR) to the dialyzed SSB^{G26C}. Adjust the volume to keep the final volume of dimethyl sulfoxide below 5% (v/v) in the reaction.
4. Perform the labeling reaction at 4°C for 4 h in the dark. Stop the reaction by adding DTT to a final concentration of 1 m*M*.
5. Remove unreacted free dye from the reaction using a 20 mL P-10 gel filtration column (Bio-Rad, Hercules, CA), preequilibrated with 25 m*M* TrisOAc (pH 8.3), 0.5 *M* NaCl, 1 m*M* EDTA, 1 m*M* DTT and 20% (v/v) glycerol. The size of filtration column will depend on the scale of labeling reaction.
6. Collect the labeled SSB fractions, which elute first, and dialyze against buffer containing 25 m*M* TrisOAc (pH 8.3), 0.5 *M* NaCl, 1 m*M* EDTA, 1 m*M* DTT, and 50% (v/v) glycerol with at least two changes of at least a 10× volume each of buffer for at least 4 h each, or one change against at least a 100× volume.
7. Determine the concentration of labeled SSB by measuring absorbance (A) at 280 nm. Correct the measured absorbance for the contribution of absorbance from the dye at 280 nm by using the formula: $A_{\text{protein}} = A_{\text{measured}} - A_{\text{cf}} \times A_{\text{dye@max}}$. Use a molar extinction coefficient of 27,880 M^{-1} cm^{-1} at 280 nm for SSB protein. Similarly, use the molar extinction coefficients 72,000 M^{-1} cm^{-1} (at 493 nm) and 112,000 $M^{-1}cm^{-1}$ (at 556 nm) for AF488 and AF546 dyes, respectively, provided by the manufacturer. Apply a correction factor (A_{cf}) of 0.11

and 0.12 for AF 488 and AF 546, respectively, for dye absorption at 280 nm.

8. Calculate degree of labeling from the moles of dye incorporated per mole of protein and store protein at −80°C. Usually, the calculated degree of labeling for SSB ranges from ~0.8 to 1.0 dye/monomer. A comparison of unlabeled and labeled enzyme by SDS-PAGE is recommended to ensure that the concentration of protein is accurate, as the presence of free dye will interfere with any spectroscopic quantification.

4. INSTRUMENT

The flow cell design, flow cell fabrication, laser trapping, microfluidic system, and temperature control system are essential and unique components of every single-molecule instrument. A detailed description of these factors is beyond the scope of this chapter. However, this information is covered in detail elsewhere (Amitani et al., 2010; Forget et al., 2013). A brief explanation of the flow cell needed, and instrumentation used, for the TIRF imaging method described herein is provided.

4.1 TIRF Flow Cell Construction

One of the most important considerations when imaging fluorescent proteins by TIRF is to prevent nonspecific binding of the proteins to the surface to which the DNA is attached. Unfortunately, the extent of nonspecific binding by fluorescent proteins can only be empirically determined. Nonetheless, common to every procedure is the scrupulous cleaning of the surface that will be imaged by TIRF. There are several published methods for cleaning, functionalizing, and passivating cover glass that can be used to immobilize DNA and minimize protein adsorption to the surface (Bell, Liu, & Kowalczykowski, 2015; Bell et al., 2012; Chandradoss et al., 2014; Forget & Kowalczykowski, 2012; Gibb, Silverstein, Finkelstein, & Greene, 2012; Jain, Liu, Xiang, & Ha, 2012; Rad et al., 2015; Rasnik, McKinney, & Ha, 2005; Zhuang et al., 2000). These methods differ in their labor intensity and longevity (Rasnik et al., 2005). Alternative surface treatments include biotinylated BSA (Bell et al., 2012, 2015; Forget & Kowalczykowski, 2012; Rad et al., 2015), PEG (Chandradoss et al., 2014; Jain et al., 2012; Zhuang et al., 2000), and lipid bilayers (Gibb et al., 2012).

There are various methods to produce TIRF flowcells compatible with an inverted microscope (Amitani et al., 2010; Forget et al., 2013). The

following procedure describes how to construct TIRF flowcells by sandwiching double-sided tape between a precleaned slide and a coverslip allowing objective-type TIRF to be conducted. Here, biotinylated BSA is used to coat the cover glass, providing stable anchor points for the biotinylated λ DNA when linked via streptavidin (Fig. 3A). The entire surface modification procedure is performed at room temperature (~22°C) (Fig. 3B).

1. Clean glass coverslips, thickness No. 1 (Fisher 22 × 22 × (0.13–0.17) mm), using a chemical etching process by sonicating them in a solution of 1 *M* KOH in methanol, for 1 h (Branson 1510 Ultrasonic Cleaner, 40 kHz), followed by sequential rinsing with reagent grade water (Barnstead Nanopure or Millipore Milli-Q) and methanol.
2. Cut channels into double-sided tape (3M™ Adhesive Transfer Tape 9437) using a RoboCutter (Craft ROBO, Graphtec). The number of channels will depend on the channel dimensions required. For this particular design, each flow channel measured 3 × 13 mm in width and length, respectively, and 58 μm (2.3 mils) deep (tape thickness).
3. Create holes for inlets and outlets in the glass slides (Fisher Scientific 25 × 75 × 1 mm) using a laser engraver (30-Watt mini, Epilog Laser). The slides were subsequently submerged in 2% (v/v) Hellmanex II (Hellma) overnight. Rigorous cleaning of the slide is unnecessary as it is relatively far from the imaging plane.
4. Attach PEEK tubing (0.5-mm inner diameter, Upchurch Scientific) to each of the etched holes using a 5-min epoxy (Devcon) to create ports.
5. Align the channels on the tape with the inlets and outlets on the slide and then place the coverslip over the area to create channels.
6. Functionalize the flow cell by sequential exposure to several solutions, using either a pipette or a syringe.
7. Immediately prior to use, using a syringe pump (KD Scientific, Holliston, MA), wash each channel with 1 *M* NaOH (degassed) for 30 min and rinse with 1 mL reagent grade water (Barnstead Nanopure or Millipore Milli-Q) (degassed), before equilibration with the appropriate buffer (e.g., 25 m*M* TrisOAc (pH 7.5), and 50 m*M* NaCl—also degassed).
8. Subsequently, inject 100 μL of 1 mg/mL biotinylated BSA (Thermo Scientific), in the same buffer (25 m*M* TrisOAc (pH 7.5), and 50 m*M* NaCl), to coat the flow cell. At this relatively high concentration of BSA, it is particularly important to be careful to avoid bubbles. Wash with 1 mL of buffer.

9. Inject 100 μL of 0.1 mg/mL streptavidin (Promega, stored at −20°C as 5 mg/mL aliquots dissolved in 25 m*M* TrisOAc (pH 7.5)) diluted in the experimentation buffer. Incubate for 10 min, and wash out free streptavidin with desired reaction buffer (1 mL).
10. Finally, the flow channel can be further passivated using Roche Blocking Reagent at 1.5 mg/mL (100 μL), dissolved in the same buffer as step 9, for 5 min.
11. Multiple channels can be prepared for use on the same day, but ensure that the channels remain solvated. This can be achieved by placing a pipette tip into the inlet and outlet and filling with buffer to act as reservoir. Proceed to Section 6.2.

4.2 TIRF Instrument

Visualization of DNA unwinding by RecQ was performed on an Eclipse TE2000U inverted microscope with a TIRF attachment (Nikon). Excitation is by a 488-nm (Picarro, 25 mW) or 561-nm (Cobolt, 25 mW) lasers, and the power measured at the objective lens is ∼2–3 and ∼5.5 mW, respectively. Fluorescence emission was detected and separated into 515 nm (30-nm bandpass) and 600 nm (40-nm bandpass) components (Optical Insights). Images were captured on a DU-897E iXon CCD camera (iXon+, Andor) and processed using Andor iQ software v. 2.4 (Amitani et al., 2010) (Fig. 3D).

5. IMAGING DNA UNWINDING BY AN INDIVIDUAL RecBCD ENZYME ON A SINGLE MOLECULE OF DNA

Briefly, the steps involved in visualizing DNA helicases or translocases on single-DNA molecules in experiments using an optical trap are (1) preparing DNA–bead complexes typically with bound protein; (2) delivery of appropriate buffers into the individual channels of a multichannel flowcell; (3) capturing a DNA–bead complex within the optical trap; and (4) moving DNA–bead complex to a channel with ATP to start the reaction and to capture images in real time.

5.1 DNA Unwinding Measured by Displacement of a Fluorescent Dye From DNA

To visualize DNA unwinding by an individual enzyme (Bianco et al., 2001; Liu et al., 2013; Spies et al., 2003), a YOYO-1-stained DNA–bead complex, to which RecBCD enzyme was bound, is optically trapped in the absence of ATP (Fig. 1B). To initiate DNA unwinding, the complex

is then moved to the reaction channel that contains ATP (Fig. 1A). DNA unwinding and degradation, and concomitant RecBCD translocation, are seen as a shortening of DNA length with time (Fig. 1C).

1. Prepare single-molecule buffer containing 50 m*M* $NaHCO_3$ (pH 8.3), 15% sucrose (w/v), and 50 m*M* DTT (SMB1); degas at least for 1 h.

   Note: We routinely perform overnight degassing of buffer containing no DTT and degas for 1 h after addition of DTT. Removal of oxygen by degassing is to reduce oxygen-mediated photobleaching and cleavage of DNA.
2. Prepare DNA–bead complexes by mixing 1 μL (~35 p*M*) of streptavidin-coated polystyrene beads (1.0 μm, Bangs Laboratories, Fishers, IN), 1 μL of 100 m*M* $NaHCO_3$ (pH 8.3), and 2 μL of 100 p*M* biotinylated λ DNA for 30 min at 37°C. The ratio between the bead and DNA may need to be varied to obtain ~1 DNA molecule to each bead.
3. Stain DNA with fluorescent dye by adding 500 μL of SMB1 containing 20 n*M* YOYO-1 (Invitrogen, Carlsbad, CA) to the bead–DNA complexes. The dye to DNA (in base pairs) ratio can be varied from 1:1 to 1:5 (Eggleston et al., 1996).
4. Flush the syringes, tubing and, flow cell with water, followed by SMB1 containing 1 mg/mL BSA (typically, at a flow rate of 800 μL/h). BSA is used as a blocking agent to prevent nonspecific binding of reaction components to the syringe, tubing, and flowcell.
5. Add 2 m*M* $Mg(OAc)_2$ and 60 n*M* of RecBCD to the YOYO-1-stained DNA–bead complexes; immediately load this solution into the syringe for the first channel.
6. Prepare 500 μL SMB1 containing 2 m*M* $Mg(OAc)_2$, and ATP at desired concentration (typically, 1 m*M*); load this solution into the syringe for the second channel.
7. Start the syringe pump to inject solution into the flow cell at a flow rate of 800 μL/h; over the course of 5–10 min, decrease the flow rate stepwise to 50 μL/h.
8. Trap a DNA–bead–RecBCD complexes in first channel and move immediately into the ATP-containing reaction channel.
9. The unwinding of dsDNA is manifested by the shortening of YOYO-1 bound DNA (Movie 1 (http://dx.doi.org/10.1016/bs.mie.2016.09.010)).

5.2 Direct Observation of Translocation on DNA by an Individual RecBCD Enzyme Conjugated to a Nanoparticle

The translocation behavior of individual RecBCD molecules can also be monitored by direct visualization of fluorescently labeled RecBCD

(Handa et al., 2005). In this method, the optically trapped DNA–bead complex containing fluorescently labeled RecBCD enzyme at the free end is moved into the ATP-containing channel and the movement of fluorescently labeled RecBCD enzyme is tracked.

1. Prepare single-molecule buffer and wash all the channels as described in Section 5.1, step 4.
2. Prepare DNA–bead complexes as described in Section 5.1, step 2.
3. Label biotinylated RecBCD using a fluorescent nanoparticle as described in Section 3.1.
4. Mix 3 μL DNA–bead and 7.8 μL of RecBCD–nanoparticle complexes together, add 2 m*M* $Mg(OAc)_2$, and incubate for 2 min.
5. Add the nanoparticle–RecBCD–DNA–bead complex into 500 μL of degassed sample buffer containing 45 m*M* $NaHCO_3$ (pH 8.2), 20% (w/v) sucrose, 50 m*M* dithiothreitol, 2 m*M* magnesium acetate, and 0.5% (v/v) blocking solution (B-10710, Molecular Probes), and load into the first channel.
6. Load single-molecule buffer containing 1 m*M* ATP, 2 m*M* $Mg(OAc)_2$, and 0.5% (v/v) blocking solution (B-10710, Molecular Probes) into the second channel.
7. Trap a nanoparticle–RecBCD–DNA–bead complex and move into second channel. The fluorescent particle is seen to move toward the trapped bead as RecBCD enzyme translocates on the DNA (Fig. 2 and Movie 2 (http://dx.doi.org/10.1016/bs.mie.2016.09.010)).

6. MEASURING DNA UNWINDING BY IMAGING FORMATION OF FLUORESCENT SSB–ssDNA COMPLEXES

The use of AF488-SSB^{G26C} as an effective biosensor for tracking helicase activity was demonstrated recently for RecQ (Rad et al., 2015); alternatively, AF546-SSB^{G26C} can also be used. The following procedure describes the method used to measure DNA unwinding of doubly tethered λ DNA on a biotin-BSA surface using a fluorescent SSB to directly detect ssDNA formation (Fig. 4C).

6.1 Immobilization and Visualization of DNA

The concentration of DNA and time required to immobilize the desired number of DNA molecules in a single field of view (80 μm × 80 μm) will depend on the surface preparation method. The three methods mentioned,

biotin-BSA PEGylation, and lipid bilayers (Sections 1.3 and 4.1) vary in their biotinylation surface density. Reactions are performed in single-molecule buffer 2 (SMB2) (25 m*M* TrisOAc (pH 7.5), 20% (w/v) sucrose, 50 m*M* DTT, and 0.1 mg/mL BSA), which had been degassed overnight in the absence of DTT (Section 5.1, step 1), unless stated otherwise.

As a guideline, for a flow channel prepared using biotin-BSA, 10–50 p*M* DNA is sufficient. The DNA (prepared as in Section 2.3) is diluted into SMB2 buffer, containing 100 n*M* YO-PRO-1 (or dye of choice, e.g., 75 n*M* Sytox Orange (Rad et al., 2015)).

1. Connect the inlet of a flow cell channel to a syringe pump (KD Scientific, Holliston, MA) and wash with SMB2, allowing the BSA to passivate the inner walls and syringe.
2. Inject the DNA solution in stages that allows association between the biotin and streptavidin but prevents both ends of the DNA being attached in close proximity. Initially, inject the DNA at a volumetric flow rate of 8000 μL/h (linear flow rate = 1.7 cm/s at center of channel, specific for channel with dimensions as described in Section 4.1). The flow is temporarily stopped for 2 min, and then the DNA is restretched by resuming flow (8000 μL/h) permitting attachment of the other end. This process is cycled until the desired number of DNA molecules has been reached.
3. Remove free DNA and stain the bound DNA by flowing in 100 vols (~200 μL) of 100 n*M* YO-PRO-1 in SMB2.
4. Acquire an image of each individual doubly tethered DNA molecule for subsequent measurement and normalization of DNA unwinding measurements.
5. The DNA can be destained if it interferes with helicase function. YO-PRO-1 is removed by washing with 200 m*M* NaCl in SMB2.
6. For a protocol specific to RecQ, the syringe is loaded with 50 μL of reaction mixture, 40–150 n*M* RecQ, 60 n*M* (monomer) AF488-SSB^{G26C}, 1 m*M* ATP, and 1 m*M* $Mg(OAc)_2$ in SMB2 to initiate the reaction. The flow required to fully stretch the DNA attached to the surface amounts to only ~0.1–0.5 pN (Bell et al., 2015).
7. For doubly tethered DNA, stop the flow.
8. Capture images every 2 s (or as appropriated for the rate of unwinding) at reduced laser power (e.g., 10–20% for our instrument; Section 4.2) to minimize photobleaching, using exposure of only ~200 ms.
9. Analyze data as described in Section 7.2.

10. Data using this method shows that RecQ can bind and start unwinding randomly on the tethered λ DNA (Movie 3 (http://dx.doi.org/10.1016/bs.mie.2016.09.010)). The individual events were each highlighted by tracks of fluorescently labeled SSB (Fig. 4A). Visualization shows different ssDNA intermediates, depending on whether RecQ had started unwinding from an end, a nick or melting of an intact duplex region (Fig. 4B). Using SYTOX Orange, instead of YO-PRO-1, and AF488-SSB^{G26C} enables both ssDNA and dsDNA to be visualized simultaneously, provided that the microscope is equipped with a Dual-View accessory (Optical Insights, LLC) (Movie 4 (http://dx.doi.org/10.1016/bs.mie.2016.09.010)).

6.2 Experimental Considerations Specific to Imaging With SSB Protein

Ordinarily, at the concentrations of SSB used, the rate of SSB association will be significantly faster than any helicase unwinding rate. Therefore, it is prudent to determine the effect of SSB concentration on the DNA unwinding rates, at each solution condition examined.

In general, the potential melting of duplex DNA by the specific SSB protein should always be considered when measuring initiation events in the presence of SSB. The eukaryotic ssDNA-bind protein, RPA (replication protein-A), induces DNA unwinding under low ionic strength conditions, especially at high concentrations of protein (Georgaki, Strack, Podust, & Hubscher, 1992; Treuner, Ramsperger, & Knippers, 1996); therefore, care must be taken to attribute initiation events to the helicase and not to the SSB. This can be easily tested with the fluorescent SSB by omitting the helicase.

It is also important to be aware that SSB-coated ssDNA is condensed compared to the contour length of naked ssDNA (Bell et al., 2015). However, by using double-tethers, thereby constraining the DNA, if the starting apparent length of the dsDNA is known, then the length of ssDNA produced can be calculated, to a good approximation, by assuming the lengths of dsDNA and SSB-coated ssDNA are equivalent (Section 7.2). A more accurate method is to calibrate the length of SSB–ssDNA complexes independently, either by fluorescent or by force measurements (Bell et al., 2015). Such steps become relevant when performing unwinding experiments in various solution conditions, as dsDNA length and the extent to which SSB-coated ssDNA condenses are dependent on the mono- and divalent-salt concentration (Bell et al., 2015).

One disadvantage of this assay, however, is that some helicases require a free ssDNA tail as a loading site to initiate unwinding. Clearly, if the SSB blocks this critical binding, then this approach for visualizing DNA unwinding cannot be used.

7. DATA ANALYSIS

7.1 Automatic DNA Length Measurement

To measure the length of fluorescent, dye-bound DNA or DNA bound with a fluorescent protein, we developed several plug-ins for automated analysis using Image J software. These were described previously (Amitani et al., 2010) and are available upon request.

7.2 Unwinding Analysis for the Fluorescent SSB-Binding Method, Using TIRF Microscopy

Time-lapse images collected during each experiment are first compiled into a stack. Then using Andor iQ software v. 2.4., to improve signal to noise, the stack is divided into groups of four frames, and each group is averaged using the built-in "lumped average" algorithm. The resultant stack contains images corresponding to 8 s time intervals, sufficient to define individual unwinding events for RecQ. For each molecule of interest, a kymograph is created in ImageJ using a line width of 1 pixel; an example is shown in Fig. 4B. Further analysis on the kymograph is conducted in ImageJ v. 1.44c (Schneider, Rasband, & Eliceiri, 2012), using the Point Picker plug-in to mark the position of the individual unwinding forks. The progression of multiple unwinding forks on the same DNA molecule can be monitored using this method. The distance from the point of initiation to the furthest point of continual fluorescent SSB signal defines unwinding track length in pixels. To determine the rate of unwinding in base pairs, a two-stage normalization procedure is required. First, for the particular camera used to acquire the images, measurements are converted into distance (in nanometers) using the calibrated camera resolution, in this instance 163.9 nm/pixel. Second, to convert nanometers into base pairs, the distance is normalized using the initial and expected lengths of the DNA molecule, outlined earlier; this can depend on the particular buffer condition. The measured length of the unwinding track is divided by the end-to-end distance of the doubly attached dsDNA molecule prior to starting the reaction. This serves as an internal normalization factor for each molecule. The length

of the λ DNA (in nanometers) at the start of the reaction is equivalent to 48,502 bp. Therefore, the ratio of fluorescent SSB track and full-length λ DNA yields the unwound length in base pairs. Finally, the rate of unwinding is obtained from fitting to the linear region of a distance vs time trace.

ACKNOWLEDGMENTS

We particularly thank Ichiro Amitani, Nev Gilhooly, Anna Kalashnikova, Katsumi Morimatsu, and Artem Lada for their comments on this manuscript, and all of the lab members, including alumni of the Kowalczykowski lab, for their contributions to this research. Funding on this research work was supported by the grants from National Institutes of Health, GM-62653 and GM-64745, to S.C.K.

REFERENCES

Akerman, B., & Tuite, E. (1996). Single- and double-strand photocleavage of DNA by YO, YOYO and TOTO. *Nucleic Acids Research*, *24*(6), 1080–1090.

Amitani, I., Baskin, R. J., & Kowalczykowski, S. C. (2006). Visualization of Rad54, a chromatin remodeling protein, translocating on single DNA molecules. *Molecular Cell*, *23*(1), 143–148. http://dx.doi.org/10.1016/j.molcel.2006.05.009.

Amitani, I., Liu, B., Dombrowski, C. C., Baskin, R. J., & Kowalczykowski, S. C. (2010). Watching individual proteins acting on single molecules of DNA. *Methods in Enzymology*, *472*, 261–291. http://dx.doi.org/10.1016/S0076-6879(10)72007-3.

Axelrod, D. (1989). Total internal reflection fluorescence microscopy. *Methods in Cell Biology*, *30*, 245–270.

Bell, J. C., Liu, B., & Kowalczykowski, S. C. (2015). Imaging and energetics of single SSB-ssDNA molecules reveal intramolecular condensation and insight into RecOR function. *Elife*, *4*, e08646. http://dx.doi.org/10.7554/eLife.08646.

Bell, J. C., Plank, J. L., Dombrowski, C. C., & Kowalczykowski, S. C. (2012). Direct imaging of RecA nucleation and growth on single molecules of SSB-coated ssDNA. *Nature*, *491*(7423), 274–278. http://dx.doi.org/10.1038/nature11598.

Bianco, P. R., Brewer, L. R., Corzett, M., Balhorn, R., Yeh, Y., Kowalczykowski, S. C., & Baskin, R. J. (2001). Processive translocation and DNA unwinding by individual RecBCD enzyme molecules. *Nature*, *409*(6818), 374–378. http://dx.doi.org/10.1038/35053131.

Bustamante, C., Bryant, Z., & Smith, S. B. (2003). Ten years of tension: Single-molecule DNA mechanics. *Nature*, *421*(6921), 423–427. http://dx.doi.org/10.1038/nature01405.

Byrd, A. K., & Raney, K. D. (2012). Superfamily 2 helicases. *Frontiers in Bioscience (Landmark edition)*, *17*, 2070–2088.

Byrd, A. K., & Raney, K. D. (2015). Fine tuning of a DNA fork by the RecQ helicase. *Proceedings of the National Academy of Sciences of the United States of America*, *112*(50), 15263–15264. http://dx.doi.org/10.1073/pnas.1520119112.

Cejka, P., & Kowalczykowski, S. C. (2010). The full-length *Saccharomyces cerevisiae* Sgs1 protein is a vigorous DNA helicase that preferentially unwinds Holliday junctions. *Journal of Biological Chemistry*, *285*(11), 8290–8301. http://dx.doi.org/10.1074/jbc.M109.083196.

Chakraborty, A., Wang, D., Ebright, Y. W., & Ebright, R. H. (2010). Azide-specific labeling of biomolecules by Staudinger-Bertozzi ligation phosphine derivatives of fluorescent probes suitable for single-molecule fluorescence spectroscopy. *Methods in Enzymology*, *472*, 19–30. http://dx.doi.org/10.1016/S0076-6879(10)72018-8.

Chandradoss, S. D., Haagsma, A. C., Lee, Y. K., Hwang, J. H., Nam, J. M., & Joo, C. (2014). Surface passivation for single-molecule protein studies. *Journal of Visualized Experiments*. *86*. , http://dx.doi.org/10.3791/50549.

Chu, W. K., & Hickson, I. D. (2009). RecQ helicases: Multifunctional genome caretakers. *Nature Reviews Cancer*, *9*(9), 644–654. http://dx.doi.org/10.1038/nrc2682.

Courcelle, J., & Hanawalt, P. C. (1999). RecQ and RecJ process blocked replication forks prior to the resumption of replication in UV-irradiated Escherichia coli. *Molecular and General Genetics*, *262*(3), 543–551.

Dillingham, M. S., & Kowalczykowski, S. C. (2008). RecBCD enzyme and the repair of double-stranded DNA breaks. *Microbiology and Molecular Biology Reviews*, *72*(4), 642–671. http://dx.doi.org/10.1128/MMBR.00020-08.

Dillingham, M. S., Spies, M., & Kowalczykowski, S. C. (2003). RecBCD enzyme is a bipolar DNA helicase. *Nature*, *423*(6942), 893–897. http://dx.doi.org/10.1038/nature01673.

Dillingham, M. S., Tibbles, K. L., Hunter, J. L., Bell, J. C., Kowalczykowski, S. C., & Webb, M. R. (2008). Fluorescent single-stranded DNA binding protein as a probe for sensitive, real-time assays of helicase activity. *Biophysical Journal*, *95*(7), 3330–3339. http://dx.doi.org/10.1529/biophysj.108.133512.

Dixon, D. A., & Kowalczykowski, S. C. (1993). The recombination hotspot χ is a regulatory sequence that acts by attenuating the nuclease activity of the E. coli RecBCD enzyme. *Cell*, *73*(1), 87–96.

Eggleston, A. K., Rahim, N. A., & Kowalczykowski, S. C. (1996). A helicase assay based on the displacement of fluorescent, nucleic acid-binding ligands. *Nucleic Acids Research*, *24*(7), 1179–1186.

Fili, N., Mashanov, G. I., Toseland, C. P., Batters, C., Wallace, M. I., Yeeles, J. T., … Molloy, J. E. (2010). Visualizing helicases unwinding DNA at the single molecule level. *Nucleic Acids Research*, *38*(13), 4448–4457. http://dx.doi.org/10.1093/nar/gkq173.

Finkelstein, I. J., Visnapuu, M. L., & Greene, E. C. (2010). Single-molecule imaging reveals mechanisms of protein disruption by a DNA translocase. *Nature*, *468*(7326), 983–987. http://dx.doi.org/10.1038/nature09561.

Forget, A. L., Dombrowski, C. C., Amitani, I., & Kowalczykowski, S. C. (2013). Exploring protein-DNA interactions in 3D using in situ construction, manipulation and visualization of individual DNA dumbbells with optical traps, microfluidics and fluorescence microscopy. *Nature Protocols*, *8*(3), 525–538. http://dx.doi.org/10.1038/nprot.2013.016.

Forget, A. L., & Kowalczykowski, S. C. (2012). Single-molecule imaging of DNA pairing by RecA reveals a three-dimensional homology search. *Nature*, *482*(7385), 423–427. http://dx.doi.org/10.1038/nature10782.

Galletto, R., Amitani, I., Baskin, R. J., & Kowalczykowski, S. C. (2006). Direct observation of individual RecA filaments assembling on single DNA molecules. *Nature*, *443*(7113), 875–878. http://dx.doi.org/10.1038/nature05197.

Georgaki, A., Strack, B., Podust, V., & Hubscher, U. (1992). DNA unwinding activity of replication protein A. *FEBS Letters*, *308*(3), 240–244.

George, J. W., Ghate, S., Matson, S. W., & Besterman, J. M. (1992). Inhibition of DNA helicase II unwinding and ATPase activities by DNA-interacting ligands. Kinetics and specificity. *Journal of Biological Chemistry*, *267*(15), 10683–10689.

Gibb, B., Silverstein, T. D., Finkelstein, I. J., & Greene, E. C. (2012). Single-stranded DNA curtains for real-time single-molecule visualization of protein-nucleic acid interactions. *Analytical Chemistry*, *84*(18), 7607–7612. http://dx.doi.org/10.1021/ac302117z.

Gilhooly, N. S., Gwynn, E. J., & Dillingham, M. S. (2013). Superfamily 1 helicases. *Frontiers in Bioscience (Scholar Edition)*, *5*, 206–216.

Greenleaf, W. J., Woodside, M. T., & Block, S. M. (2007). High-resolution, single-molecule measurements of biomolecular motion. *Annual Review of Biophysics and Biomolecular Structure*, *36*, 171–190. http://dx.doi.org/10.1146/annurev.biophys.36.101106.101451.

Ha, T., Kozlov, A. G., & Lohman, T. M. (2012). Single-molecule views of protein movement on single-stranded DNA. *Annual Review of Biophysics*, *41*, 295–319. http://dx.doi.org/10.1146/annurev-biophys-042910-155351.

Handa, N., Bianco, P. R., Baskin, R. J., & Kowalczykowski, S. C. (2005). Direct visualization of RecBCD movement reveals cotranslocation of the RecD motor after χ recognition. *Molecular Cell*, *17*(5), 745–750. http://dx.doi.org/10.1016/j.molcel. 2005.02.011.

Handa, N., Morimatsu, K., Lovett, S. T., & Kowalczykowski, S. C. (2009). Reconstitution of initial steps of dsDNA break repair by the RecF pathway of *E. coli*. *Genes and Development*, *23*(10), 1234–1245. http://dx.doi.org/10.1101/gad.1780709.

Harmon, F. G., & Kowalczykowski, S. C. (1998). RecQ helicase, in concert with RecA and SSB proteins, initiates and disrupts DNA recombination. *Genes and Development*, *12*(8), 1134–1144.

Harmon, F. G., & Kowalczykowski, S. C. (2000). Coupling of DNA helicase function to DNA strand exchange activity. *Methods in Molecular Biology*, *152*, 75–89. http://dx.doi.org/10.1385/1-59259-068-3:75.

Harmon, F. G., & Kowalczykowski, S. C. (2001). Biochemical characterization of the DNA helicase activity of the *Escherichia coli* RecQ helicase. *Journal of Biological Chemistry*, *276*(1), 232–243. http://dx.doi.org/10.1074/jbc.M006555200.

Hein, B., Willig, K. I., Wurm, C. A., Westphal, V., Jakobs, S., & Hell, S. W. (2010). Stimulated emission depletion nanoscopy of living cells using SNAP-tag fusion proteins. *Biophysical Journal*, *98*(1), 158–163. http://dx.doi.org/10.1016/j.bpj.2009.09.053.

Hilario, J., Amitani, I., Baskin, R. J., & Kowalczykowski, S. C. (2009). Direct imaging of human Rad51 nucleoprotein dynamics on individual DNA molecules. *Proceedings of the National Academy of Sciences of the United States of America*, *106*(2), 361–368. http://dx.doi.org/10.1073/pnas.0811965106.

Hilario, J., & Kowalczykowski, S. C. (2010). Visualizing protein-DNA interactions at the single-molecule level. *Current Opinion in Chemical Biology*, *14*(1), 15–22. http://dx.doi.org/10.1016/j.cbpa.2009.10.035.

Honda, M., Park, J., Pugh, R. A., Ha, T., & Spies, M. (2009). Single-molecule analysis reveals differential effect of ssDNA-binding proteins on DNA translocation by XPD helicase. *Molecular Cell*, *35*(5), 694–703. http://dx.doi.org/10.1016/j.molcel.2009.07.003.

Jain, A., Liu, R., Xiang, Y. K., & Ha, T. (2012). Single-molecule pull-down for studying protein interactions. *Nature Protocols*, 7(3), 445–452. http://dx.doi.org/10.1038/nprot.2011.452.

Kapanidis, A. N., Ebright, Y. W., & Ebright, R. H. (2001). Site-specific incorporation of fluorescent probes into protein: Hexahistidine-tag-mediated fluorescent labeling with Ni(2+):nitrilotriacetic acid (n)-fluorochrome conjugates. *Journal of the American Chemical Society*, *123*(48), 12123–12125.

Kapanidis, A. N., & Strick, T. (2009). Biology, one molecule at a time. *Trends in Biochemical Sciences*, *34*(5), 234–243. http://dx.doi.org/10.1016/j.tibs.2009.01.008.

Lionnet, T., Allemand, J. F., Revyakin, A., Strick, T. R., Saleh, O. A., Bensimon, D., & Croquette, V. (2012). Single-molecule studies using magnetic traps. *Cold Spring Harbor Protocols*, *2012*(1), 34–49. http://dx.doi.org/10.1101/pdb.top067488.

Liu, B., Baskin, R. J., & Kowalczykowski, S. C. (2013). DNA unwinding heterogeneity by RecBCD results from static molecules able to equilibrate. *Nature*, *500*(7463), 482–485. http://dx.doi.org/10.1038/nature12333.

Liu, J., Qian, N., & Morrical, S. W. (2006). Dynamics of bacteriophage T4 presynaptic filament assembly from extrinsic fluorescence measurements of Gp32-single-stranded DNA interactions. *Journal of Biological Chemistry*, *281*(36), 26308–26319. http://dx.doi.org/10.1074/jbc.M604349200.

Lohman, T. M., & Ferrari, M. E. (1994). Escherichia coli single-stranded DNA-binding protein: Multiple DNA-binding modes and cooperativities. *Annual Review of Biochemistry*, *63*, 527–570. http://dx.doi.org/10.1146/annurev.bi.63.070194.002523.

Lohman, T. M., Tomko, E. J., & Wu, C. G. (2008). Non-hexameric DNA helicases and translocases: Mechanisms and regulation. *Nature Reviews. Molecular Cell Biology*, *9*(5), 391–401. http://dx.doi.org/10.1038/nrm2394.

Manosas, M., Xi, X. G., Bensimon, D., & Croquette, V. (2010). Active and passive mechanisms of helicases. *Nucleic Acids Research*, *38*(16), 5518–5526. http://dx.doi.org/10.1093/nar/gkq273.

Moffitt, J. R., Chemla, Y. R., Smith, S. B., & Bustamante, C. (2008). Recent advances in optical tweezers. *Annual Review of Biochemistry*, 77, 205–228. http://dx.doi.org/10.1146/annurev.biochem.77.043007.090225.

Morimatsu, K., & Kowalczykowski, S. C. (2014). RecQ helicase and RecJ nuclease provide complementary functions to resect DNA for homologous recombination. *Proceedings of the National Academy of Sciences of the United States of America*, *111*(48), E5133–E5142. http://dx.doi.org/10.1073/pnas.1420009111.

Neuman, K. C., & Nagy, A. (2008). Single-molecule force spectroscopy: Optical tweezers, magnetic tweezers and atomic force microscopy. *Nature Methods*, *5*(6), 491–505. http://dx.doi.org/10.1038/nmeth.1218.

Nimonkar, A. V., Amitani, I., Baskin, R. J., & Kowalczykowski, S. C. (2007). Single molecule imaging of Tid1/Rdh54, a Rad54 homolog that translocates on duplex DNA and can disrupt joint molecules. *Journal of Biological Chemistry*, *282*(42), 30776–30784. http://dx.doi.org/10.1074/jbc.M704767200.

Perkins, T. T., Quake, S. R., Smith, D. E., & Chu, S. (1994). Relaxation of a single DNA molecule observed by optical microscopy. *Science*, *264*(5160), 822–826.

Perkins, T. T., Smith, D. E., & Chu, S. (1994). Direct observation of tube-like motion of a single polymer chain. *Science*, *264*(5160), 819–822.

Pyle, A. M. (2008). Translocation and unwinding mechanisms of RNA and DNA helicases. *Annual Review of Biophysics*, *37*, 317–336. http://dx.doi.org/10.1146/annurev.biophys.37.032807.125908.

Qi, Z., & Greene, E. C. (2016). Visualizing recombination intermediates with single-stranded DNA curtains. *Methods*, *105*, 62–74. http://dx.doi.org/10.1016/j.ymeth.2016.03.027.

Rad, B., Forget, A. L., Baskin, R. J., & Kowalczykowski, S. C. (2015). Single-molecule visualization of RecQ helicase reveals DNA melting, nucleation, and assembly are required for processive DNA unwinding. *Proceedings of the National Academy of Sciences of the United States of America*, *112*(50), E6852–E6861. http://dx.doi.org/10.1073/pnas.1518028112.

Rad, B., & Kowalczykowski, S. C. (2012a). Efficient coupling of ATP hydrolysis to translocation by RecQ helicase. *Proceedings of the National Academy of Sciences of the United States of America*, *109*(5), 1443–1448. http://dx.doi.org/10.1073/pnas.1119952109.

Rad, B., & Kowalczykowski, S. C. (2012b). Translocation of E. coli RecQ helicase on single-stranded DNA. *Biochemistry*, *51*(13), 2921–2929. http://dx.doi.org/10.1021/bi3000676.

Raghunathan, S., Kozlov, A. G., Lohman, T. M., & Waksman, G. (2000). Structure of the DNA binding domain of E. coli SSB bound to ssDNA. *Nature Structural Biology*, *7*(8), 648–652. http://dx.doi.org/10.1038/77943.

Rasnik, I., McKinney, S. A., & Ha, T. (2005). Surfaces and orientations: Much to FRET about? *Accounts of Chemical Research*, *38*(7), 542–548. http://dx.doi.org/10.1021/ar040138c.

Reuter, M., Parry, F., Dryden, D. T., & Blakely, G. W. (2010). Single-molecule imaging of Bacteroides fragilis AddAB reveals the highly processive translocation of a single motor helicase. *Nucleic Acids Research*, *38*(11), 3721–3731. http://dx.doi.org/10.1093/nar/gkq100.

Richard, D. J., Bolderson, E., & Khanna, K. K. (2009). Multiple human single-stranded DNA binding proteins function in genome maintenance: Structural, biochemical and functional analysis. *Critical Reviews in Biochemistry and Molecular Biology*, *44*(2–3), 98–116. http://dx.doi.org/10.1080/10409230902849180.

Roman, L. J., Eggleston, A. K., & Kowalczykowski, S. C. (1992). Processivity of the DNA helicase activity of Escherichia coli recBCD enzyme. *Journal of Biological Chemistry*, *267*(6), 4207–4214.

Roman, L. J., & Kowalczykowski, S. C. (1989). Characterization of the helicase activity of the *Escherichia coli* RecBCD enzyme using a novel helicase assay. *Biochemistry*, *28*(7), 2863–2873.

Roy, R., Hohng, S., & Ha, T. (2008). A practical guide to single-molecule FRET. *Nature Methods*, *5*(6), 507–516. http://dx.doi.org/10.1038/nmeth.1208.

Sarlos, K., Gyimesi, M., & Kovacs, M. (2012). RecQ helicase translocates along single-stranded DNA with a moderate processivity and tight mechanochemical coupling. *Proceedings of the National Academy of Sciences of the United States of America*, *109*(25), 9804–9809. http://dx.doi.org/10.1073/pnas.1114468109.

Schneider, C. A., Rasband, W. S., & Eliceiri, K. W. (2012). NIH Image to ImageJ: 25 years of image analysis. *Nature Methods*, *9*(7), 671–675.

Shaner, N. C., Steinbach, P. A., & Tsien, R. Y. (2005). A guide to choosing fluorescent proteins. *Nature Methods*, *2*(12), 905–909. http://dx.doi.org/10.1038/nmeth819.

Shereda, R. D., Kozlov, A. G., Lohman, T. M., Cox, M. M., & Keck, J. L. (2008). SSB as an organizer/mobilizer of genome maintenance complexes. *Critical Reviews in Biochemistry and Molecular Biology*, *43*(5), 289–318. http://dx.doi.org/10.1080/10409230802341296.

Singleton, M. R., Dillingham, M. S., & Wigley, D. B. (2007). Structure and mechanism of helicases and nucleic acid translocases. *Annual Review of Biochemistry*, *76*, 23–50. http://dx.doi.org/10.1146/annurev.biochem.76.052305.115300.

Spies, M. (2013). There and back again: New single-molecule insights in the motion of DNA repair proteins. *Current Opinion in Structural Biology*, *23*(1), 154–160. http://dx.doi.org/10.1016/j.sbi.2012.11.008.

Spies, M., Amitani, I., Baskin, R. J., & Kowalczykowski, S. C. (2007). RecBCD enzyme switches lead motor subunits in response to c recognition. *Cell*, *131*(4), 694–705. http://dx.doi.org/10.1016/j.cell.2007.09.023.

Spies, M., Bianco, P. R., Dillingham, M. S., Handa, N., Baskin, R. J., & Kowalczykowski, S. C. (2003). A molecular throttle: The recombination hotspot c controls DNA translocation by the RecBCD helicase. *Cell*, *114*(5), 647–654.

Spies, M., Dillingham, M. S., & Kowalczykowski, S. C. (2005). DNA helicases. In *McGraw-Hill yearbook of science & technology* (pp. 95–98). New York, NY: McGraw-Hill.

Sun, B., & Wang, M. D. (2016). Single-molecule perspectives on helicase mechanisms and functions. *Critical Reviews in Biochemistry and Molecular Biology*, *51*(1), 15–25. http://dx.doi.org/10.3109/10409238.2015.1102195.

Taylor, A. F., & Smith, G. R. (2003). RecBCD enzyme is a DNA helicase with fast and slow motors of opposite polarity. *Nature*, *423*(6942), 889–893. http://dx.doi.org/10.1038/nature01674.

Treuner, K., Ramsperger, U., & Knippers, R. (1996). Replication protein A induces the unwinding of long double-stranded DNA regions. *Journal of Molecular Biology*, *259*(1), 104–112. http://dx.doi.org/10.1006/jmbi.1996.0305.

Umezu, K., & Nakayama, H. (1993). RecQ DNA helicase of *Escherichia coli*. Characterization of the helix-unwinding activity with emphasis on the effect of single-stranded DNA-binding protein. *Journal of Molecular Biology*, *230*(4), 1145–1150. http://dx.doi.org/10.1006/jmbi.1993.1231.

Umezu, K., Nakayama, K., & Nakayama, H. (1990). Escherichia coli RecQ protein is a DNA helicase. *Proceedings of the National Academy of Sciences of the United States of America*, *87*(14), 5363–5367. http://dx.doi.org/10.1073/pnas.87.14.5363.

Witte, M. D., Theile, C. S., Wu, T., Guimaraes, C. P., Blom, A. E., & Ploegh, H. L. (2013). Production of unnaturally linked chimeric proteins using a combination of sortase-catalyzed transpeptidation and click chemistry. *Nature Protocols*, *8*(9), 1808–1819. http://dx.doi.org/10.1038/nprot.2013.103.

Wu, B., Piatkevich, K. D., Lionnet, T., Singer, R. H., & Verkhusha, V. V. (2011). Modern fluorescent proteins and imaging technologies to study gene expression, nuclear localization, and dynamics. *Current Opinion in Cell Biology*, *23*(3), 310–317. http://dx.doi.org/10.1016/j.ceb.2010.12.004.

Yodh, J. G., Schlierf, M., & Ha, T. (2010). Insight into helicase mechanism and function revealed through single-molecule approaches. *Quarterly Reviews of Biophysics*, *43*(2), 185–217. http://dx.doi.org/10.1017/S0033583510000107.

Zhuang, X., Bartley, L. E., Babcock, H. P., Russell, R., Ha, T., Herschlag, D., & Chu, S. (2000). A single-molecule study of RNA catalysis and folding. *Science*, *288*(5473), 2048–2051.